

Domain Formation: Decided Before, or After the Transition?

Nuno D. Antunes

*Center for Theoretical Physics, University of Sussex,
Falmer, Brighton BN1 9WJ, U.K.*

Pedro Gandra and Ray J. Rivers

*Blackett Laboratory, Imperial College
London SW7 2BZ, U.K.*

There is increasing evidence that causality provides useful bounds in determining the domain structure after a continuous transition. In devising their scaling laws for domain size after such a transition, Zurek and Kibble presented arguments in which causality is important both *before* and *after* the time at which the transition begins to be implemented. Using numerical simulations of kinks in 1+1 dimensions, we explain how the domain structure is determined exclusively by what happens *after* the transition, even though the correlation length freezes in *before* the transition.

PACS numbers: 03.70.+k, 05.70.Fh, 03.65.Yz

I. INTRODUCTION

It is inevitable that causality will provide constraints on the formation of domains after a continuous transition. Although, adiabatically, correlation lengths diverge, the finite speed at which the order parameter can adjust to the changing environment guarantees that correlation lengths remain finite for transitions implemented in finite times. Assuming that systems do change as fast as they can, Kibble [1] and Zurek [2, 3] predicted simple scaling behaviour for the maximum correlation length of the order parameters of the early universe and condensed matter systems respectively, as a function of the cooling rate.

Domain formation, the frustration of the order parameter fields, is often visible through topological defects, typically vortices, which mediate between different equivalent ground states. Since defects are, in principle, observable, they provide an excellent experimental tool for confirming this scaling behaviour, insofar as the defect separation can be correlated directly to the order parameter. Several experiments have been performed to measure defect density that support the KZ scaling behaviour under this assumption [4, 5, 6], which we term the Kibble-Zurek scenario, or are commensurate with its predictions [6, 7, 8, 9, 10].

In this paper we give a critical reappraisal of the Kibble-Zurek (KZ) scenario or, more accurately, scenarios. There are several different ways to derive causal bounds on defect densities. Although they agree numerically for simple systems, they differ conceptually in their assumption as to how the length scale that determines the defect separation arises. The main distinction is whether this is set when the system freezes in *before* the transition or when the system relaxes *after* the transition has begun.

In this paper we shall show that despite the fact that the correlation length freezes in *before* the transition, this

value does not determine the density of defects upon their appearance, contrary to the standard formulation of causal bounds. As we shall see, the defect density is determined entirely by what happens *after* the transition has begun. This latter point has been argued by one of us (RR) over many years [11, 12, 13, 14] in the context of analytic approximations and by Moro and Lythe [15] using numerical simulations to supplement similar analytic results but, we feel, can benefit from the explicit demonstration that we give here. It is also timely in that the first experiments [16] are being performed that show that the defect density depends on what happens *after* the transition. We shall turn to these in our concluding section.

II. THE KZ SCENARIOS

To be specific, consider a system with critical temperature T_c , cooled through that temperature so that, if $T(t)$ is the temperature at time t , then $T(0) = T_c$.

$$\dot{T}(0) = -T_c/\tau_Q$$

defines the quench time τ_Q . The adiabatic correlation length $\xi_{ad}(t) = \xi_{ad}(T(t))$ diverges near $t = 0$ but the true correlation length $\xi(t)$ remains finite. The standard formulation of the KZ scenario is that the correlation length ξ that characterizes the onset of order is the equilibrium correlation length $\xi = \xi_{ad}(\bar{t})$ at some appropriate time $\bar{t} < 0$ *before* the transition is implemented.

The argument goes as follows; at time t there is a maximum speed $c(T(t)) = c(t)$ at which the system can order itself. In the early universe this is the constant speed of light, in superfluid ${}^4\text{He}$, say, the speed of second sound, vanishing at $T = T_c$. [Whether there is critical slowing down or not is irrelevant.] From this we can define a relaxation time $\tau(t) = \xi_{ad}(t)/c(t)$. The earliest suggestion, due to Zurek, is that, initially, for $t < 0$ some way

before the transition, the system behaves adiabatically. However, the system freezes in (the 'impulse' region) at time $-\bar{t}$, where

$$\bar{t} \approx \tau(\bar{t}), \quad (1)$$

i.e. when the time to the transition matches the relaxation time. It is proposed that the correlation length $\bar{\xi} = \xi_{ad}(-\bar{t})$ frozen out at this time will determine the domain size at the transition.

The argument due to Kibble is even simpler; $\xi(t)$ cannot grow faster than $c(t)$. If $\xi(t) \approx \xi_{ad}(t)$ until the system cannot keep up with the cooling, the time $-\bar{t}$ at which the system freezes in is defined by the condition

$$\dot{\xi}_{ad}(-\bar{t}) \approx c(-\bar{t}). \quad (2)$$

For simple systems both estimates of \bar{t} agree, to give the allometric form [3]

$$\bar{\xi}_{<} = \xi_{ad}(-\bar{t}) = a_{<}(\tau_Q)^{\sigma_{<}}. \quad (3)$$

The scaling exponent $\sigma_{<}$ depends on the (adiabatic) critical behaviour of the system as $T \rightarrow T_c-$, and $a_{<}$ depends on the microscopic properties of the system.

In addition to considering relaxation times before the event Zurek also invoked [3] causal horizons *after* the event to obtain causal bounds. At time t the causal horizon in which the order parameter can be correlated is

$$\xi_c(t) \approx 2 \int_0^t ds c(s). \quad (4)$$

From this viewpoint our horizon bound for the earliest time \bar{t} that we can see defects is when $\xi_c(t)$ becomes larger than the coherence length $\xi_{ad}(t)$. That is, the causal horizon is big enough to hold a classical defect,

$$\xi_c(\bar{t}) = \xi_{ad}(\bar{t}). \quad (5)$$

The correlation length is then $\bar{\xi}_{>} = \xi_{ad}(\bar{t})$.

A parallel case that the relevant time for setting $\bar{\xi}$ is *after* the transition can be made for Kibble's analysis, by saying that the impulse regime will give way to the adiabatic regime once

$$\dot{\xi}_{ad}(\bar{t}) \approx -c(\bar{t}), \quad (6)$$

and it is this that determines the relevant \bar{t} . Insofar as $\xi_{ad}(t)$ is symmetric, this gives the same \bar{t} as in (2). Again, both estimates (6) and (5) for \bar{t} agree, to give

$$\bar{\xi}_{>} = a_{>}(\tau_Q)^{\sigma_{>}}, \quad (7)$$

where the scaling exponent $\sigma_{>}$ depends now on the (adiabatic) critical behaviour of the system as $T \rightarrow T_c-$.

For continuous $\dot{T}(t)$ the scaling exponents $\sigma_{<} = \sigma_{>}$ are equal, when both exist. As a result (3) and (7) are conflated as $\bar{\xi} = a(\tau_Q)^\sigma$, the KZ *scaling law*.

In either formulation Kibble and Zurek then make the second assumption, that the relevant $\bar{\xi}$ sets the initial

scale of the defect network, with defect separation $\xi_{\text{def}} \approx \bar{\xi}$.

In this paper we shall show that despite the fact that the correlation length freezes in at $\bar{\xi}$ satisfying (3), this does not fix the density of defects. Instead, the density is determined by the growth of instabilities after the transition, which essentially matches (7) without invoking causality directly, although all evolution is, inevitably, causal.

III. THE MODEL: LENGTH SCALES

We will consider a simple model in 1+1 dimensions that has been used as a first step in several studies of defect formation [17, 18]. This model is easily amenable to numerical simulation and leads to the correct scaling laws for the defect density. In a future publication we will deal with systems with larger number of spatial dimensions. Nevertheless we expect the results discussed below and the analytical estimates behind these to generalize to higher dimensions.

Specifically, we consider the following Langevin equation, describing a time-dependent Ginzburg-Landau (TDGL) field theory:

$$\partial_t^2 \phi - \nabla^2 \phi + \alpha^2 \partial_t \phi + m^2(t) \phi - 2\lambda \phi^3 = \alpha \zeta, \quad (8)$$

where ζ is a Gaussian noise term obeying

$$\langle \zeta(x', t') \zeta(x, t) \rangle = 2T \delta(x' - x) \delta(t' - t), \quad \langle \zeta(x, t) \rangle = 0. \quad (9)$$

In one dimension $\nabla^2 \phi = \partial_x^2 \phi$, α measures the amplitude of the noise, and its square quantifies the dissipative effects. This relation between the amplitudes of the noise and the dissipative term ensure that the fluctuation-dissipation condition is satisfied and that for very long times the system should eventually reach thermal equilibrium at temperature T .

This TDGL model is motivated empirically for overdamped (large α) condensed matter systems but, even in their idealised form, we would expect relativistic field theories to have non-linear noise arising from their environments. However, we have shown elsewhere that scaling behaviour is, essentially, independent of the linearity or non-linearity of the noise and we stick with (8).

We start by presenting a simplified analytic argument supporting the assumption that the correlation length does freeze in before the transition, as anticipated by Kibble and Zurek. This will also help clarifying the reason why this scale does not necessarily set the value of the final defect density. In the simplest version of the model, the mass term is decreased linearly in time from an initial positive value μ^2 as

$$m^2(t) = -\mu^2 \frac{t}{\tau_Q}, \quad -\tau_Q < t \leq 0 \quad (10)$$

For $t < -\tau_Q$ the mass term is set to constant μ^2 . For values of time larger (smaller) than τ_Q ($-\tau_Q$) the mass term is set to constant $-\mu^2$ (μ^2).

To understand how the system does freeze in at time $-\bar{t}$, for $t < 0$ non-linear excitations have not had time to grow and it is sufficient to set $\lambda = 0$ in (8). For reasons of familiarity it is convenient to extend the (now linear) equation to three space dimensions for $t < 0$. The field correlation function $G(r, t) = \langle \phi(\vec{x})\phi(\vec{0}) \rangle_t$ is expressible as

$$G(r, t) = \int \frac{d^3k}{(2\pi)^3} P(k, t) e^{i\vec{k}\cdot\vec{x}}, \quad (11)$$

where $P(k, t)$ is the *power* in the fluctuations of wave-vector \vec{k} . The solutions to (8) are given in terms of Airy functions and their generalisations, and are messy without being very informative (see [15]). It is sufficient, for illustrative purposes, to restrict ourselves to the case of strong dissipation, whereby Airy functions become exponentials. As we have shown before [19], for strong damping,

$$P(k, t) = \int_0^\infty d\tau \bar{T}(t - \tau/2) e^{-\tau k^2} e^{-\int_0^\tau d\tau' m^2(t - \tau'/2)}, \quad (12)$$

up to an irrelevant renormalisation. In turn, this gives $G_0(r, t) =$

$$= \int_0^\infty d\tau \bar{T}(t - \tau/2) \left(\frac{1}{4\pi\tau} \right)^{3/2} e^{-r^2/4\tau} e^{-\int_0^\tau d\tau' \epsilon(t - \tau'/2)}. \quad (13)$$

It is not difficult to see that, for r large enough,

$$G(r, 0) \approx \frac{1}{4\pi r} \exp[a(r/\bar{\xi}_<)^{4/3}] \quad (14)$$

in this case. In (14) $\bar{\xi}_<$ is, indeed, the correlation length that follows from (1) and (2) above and $a \approx 1$.

What is important here is that the correlation length $\bar{\xi}_<$ is determined from the position of the nearest singularity in the complex k -plane of the integral (11) after performing the angular integrations or, equivalently, from the *large-distance* behaviour of the correlation function.

The reason why, both for this and the more general case of arbitrary α , this length does not set the scale for the density of defects is that defects are identified by the field zeroes at their cores when they are formed at $t > 0$. Initially, prior to $t = 0$, there are zeroes on all scales. However, once the transition begins to get under way, the instabilities in the long wavelength modes of the field lead to exponential growth in long wavelength amplitudes that orders the fields. Insofar that we can persist with the linearized system after the transition, the separation of zeroes ξ_{zero} at the formation of defects is [20, 21]

$$\frac{1}{\xi_{zero}^2} = \frac{-1}{2\pi} \frac{G''(r=0, \bar{t})}{G'(r=0, \bar{t})}, \quad (15)$$

where dashes denote differentiation with respect to r . That is, the information comes entirely from the *short distance* behaviour of $G(r, t)$ for $t > 0$, rather than the

long-distance behaviour that determined $\bar{\xi}_<$ of (14) for $t \leq 0$. It is determined by the second moment of the power spectrum, rather than its analytic structure.

It happens that, in mean-field theory at least, ξ_{zero} of (15) can have the same scaling behaviour as $\bar{\xi}_>$ of (7), that would be obtained from (6) and (5). There are only logarithmic corrections to the scaling laws, provided thermal fluctuations, that introduce a further length scale (the Ginzburg correlation length) are unimportant [13]. The work of [15] shows just how reliable this analytic approximation is, provided transients are taken into account.

IV. NUMERICAL SIMULATIONS

For this type of quench, we expect that some time after τ_Q the field should settle to a series of alternating positive and negative vacuum regions. These regions will be separated by the topological defects of the theory, kinks and anti-kinks interpolating between the opposite vacua. The defects will then enter a regime of slow evolution with pair annihilation taking place at long times. During this stage of the evolution there is a one-to-one correspondence between kinks and anti-kinks and zeros of the scalar field ϕ , making it trivial to identify them numerically.

Depending on the value of the dissipation coefficient α^2 , we expect that the final density of defects $N_{\text{def}} = 1/\xi_{\text{def}}$ will scale with different powers of the quench time scale. For high dissipation the system is effectively first-order in time, whereas for low α the second derivative dominates the evolution and the system behaves in a relativistic fashion. Assuming that the final defect density is of the order of the inverse of the freeze-out correlation length, N_{def} should scale as $\tau_Q^{-\sigma}$. As discussed extensively in the literature and verified numerically for this model [17, 18], the exponent is given by $\sigma \simeq 1/4$ in the dissipative regime, and $\sigma \simeq 1/3$ in the relativistic case.

We will now look at variations of the quench model described above in which we modify the basic system so that the properties of the quench are qualitatively different before and after the transition takes place at $t = 0$. By measuring the final defect densities and determining the corresponding scaling powers, we will be able to determine which period of the evolution dictates the outcome. Though transitions such as envisaged here are unlikely to be realisable in a physical situation, such scenarios are useful as idealized experiments. We stress that our primary concern here is with a matter of principle, given the general acceptance of the KZ scenario in its original form. Nevertheless, as we will discuss below, experimental results in transitions in Josephson Junctions can be understood in terms of distinct behaviours of the system before and after the transition.

As already mentioned, the value of the dissipation in equation (8) determines the scaling power of the final density of defects. In the first variation we will rely on

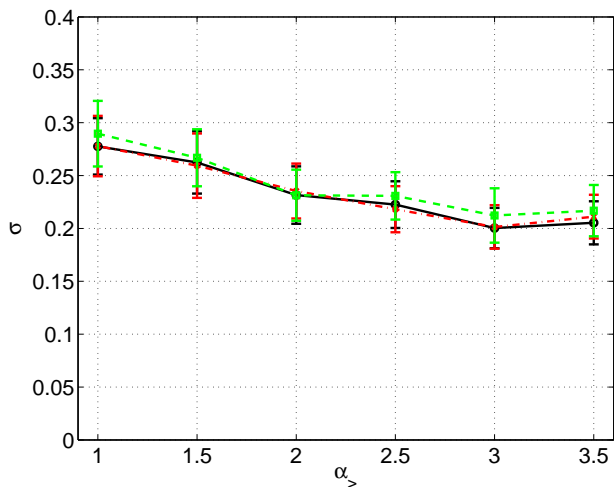


FIG. 1: Final defect density scaling power as a function of the noise amplitude for $t > 0$. The amplitude before the transition was set to $\alpha_< = 0.4$ and $\alpha_< = 0.5$ for the full and dash-dotted curves respectively. For comparison we plot (dashed curve) the standard result for a case with constant dissipation throughout the quench, *i.e.* $\alpha_< = \alpha_>$. The error bars are the standard deviation of the result over a set of 10 independent realizations of the quench.

this fact to discriminate between the effects of the two main stages of the quench on the final outcome. The idea is to allow α to take two distinct values, $\alpha = \alpha_<$ for $t < 0$ and $\alpha = \alpha_>$ for $t > 0$, characterizing the dissipation and the thermal noise before and after the transition respectively. If $\alpha_<$ and $\alpha_>$ are values typical of different regimes (under and over-damped and vice-versa) for $t < 0$ and $t > 0$ respectively, the measured value of σ should reflect the relevant period of the evolution.

The numerical procedure used in this work follows very closely that of [18]. We will outline it here briefly and refer the reader to the aforementioned publication for a more detailed description. The parameters of the potential are $\mu^2 = 1.0$ and $\lambda = 1.0$ and the bath temperature T is set to a low value, typically $T = 0.01$. For every fixed choice of $\alpha_<$ and $\alpha_>$ a set of quenches is performed with $\tau_Q = 2^n$, $n = 1, 2, \dots, 9$ and the final defect density is obtained by counting zeros of the field at a final time, defined as a multiple of τ_Q . This approach to determining the final kink number leads to slight discrepancies in the estimate of σ in the extreme high/low-dissipation cases. These are nevertheless easily controlled [17, 18] and as we will see below the accuracy obtained is more than sufficient for the needs of the present work. Finally, we perform a fit of the final defect density versus τ_Q to a power law and thus obtain the scaling exponent σ .

In Fig. 1 we show the results for a case where the evolution before the transition is well in the under-damped regime. In [18] we showed that for this specific model, the transition between the two types of evolution takes place at about $\alpha_c = 0.8$. The two values of $\alpha_< = 0.4, 0.5$ used here are both comfortably below α_c . In both cases

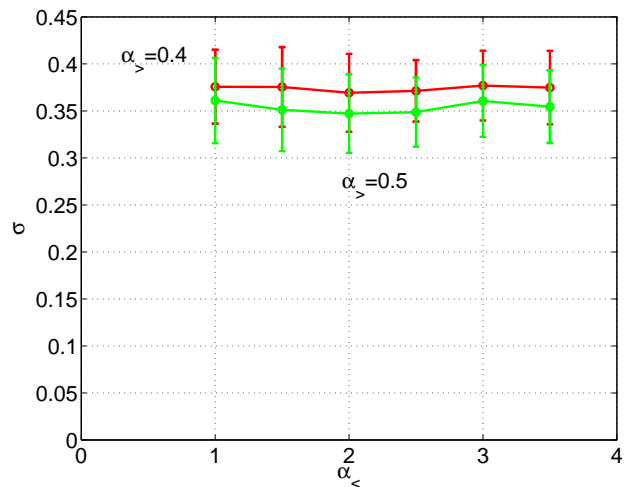


FIG. 2: Defect scaling power as a function of the noise amplitude for $t < 0$. For $t > 0$ the amplitude are $\alpha_> = 0.4$ and $\alpha_> = 0.5$. Error bars are as in Fig. 1.

we allow $\alpha_>$ to vary between 1.0 and 3.5, covering a part of the over-damped region of parameter space. As illustrated in Fig. 1 the results show clearly that the scaling parameter σ is determined exclusively by the value of $\alpha_>$. The result for the scaling exponent is unmistakably typical of the over-damped regime, despite the fact the part of the evolution was under-damped. Not only that, but the precise value of σ does not seem to be affected by $\alpha_<$. Within the error bars, the curves obtained are indistinguishable from the case where the dissipation is kept constant, and equal to $\alpha_>$, throughout the transition.

In Fig. 2 we show the results for the opposite situation. Here we kept the dissipation *after* the transition constant and in the under-damped regime, while keeping $\alpha_<$ in the over-damped region. The measured σ is constant within error bars, and has a value typical of an under-damped evolution. The values of the scaling power for a quench with constant α set to 0.4 and 0.5 are $\sigma = 0.39$ and $\sigma = 0.35$ respectively¹. As in the previous example, the values shown in Fig. 2 coincide with these. Once again this strongly suggests that the outcome is determined exclusively by the period of the quench taking place after the phase transition.

For our second example we take a more radical departure from the original model (8). While maintaining the dissipation at a constant value throughout the whole evolution, we change the rate of the quench at $t = 0$. For negative times the squared mass term $m^2(t)$ will go from μ^2 at $t = -\tau_{Q<}$ to zero at $t = 0$. For $t > 0$ an alternative quench rate is introduced, with $m^2(t)$ decreasing linearly and reaching $-\mu^2$ for $t = \tau_{Q>}$. As in the previ-

¹ Since we are working on the region of very low dissipations these are slightly larger than $1/3$, the typical value for the under-damped regime, a consequence of saturation phenomena [17, 18].

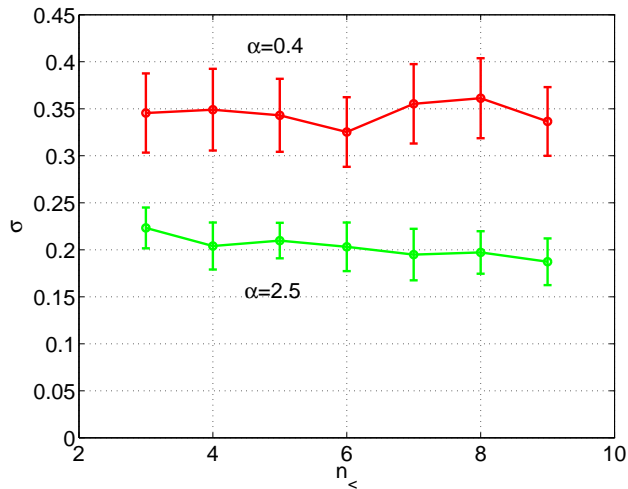


FIG. 3: Defect scaling power as a function of the fixed, $t < 0$ quench time $\tau_{Q<} = 2^{n_{<}}$, for under-damped ($\alpha = 0.4$) and over-damped ($\alpha = 2.5$) cases. Error bars are as in Fig. 1.

ous section, we expect the outcome to reflect the relative importance of the two periods of the evolution.

In Fig. 3 we show the results for two cases, with α in the under-damped and over-damped region respectively. For both sets of simulations, $\tau_{Q<}$ was kept constant at a value $\tau_{Q<} = 2^{n_{<}}$ for fixed $n_{<}$ whilst $\tau_{Q>} = 2^{n_{>}}$ was varied throughout the usual range, with $n_{>} = 1, \dots, 9$. If the final number of defects were determined by $\tau_{Q<}$ we should observe no scaling, with a constant number of defects being obtained at the end of each simulation. Instead, we found that the final density clearly scales with $\tau_{Q>}$, with a power that is determined by the magnitude of α . As seen in Fig. 3 the value of the scaling power changes very little with the quench rate at negative time. For the two choices of $\alpha = 0.4, 2.5$, the exponents for the basic quenches with $\tau_{Q<} = \tau_{Q>}$ are 0.39 and 0.23 respectively. The measured σ 's lie very near these, confirming that the $t > 0$ part of the evolution is the dominant one. As an extra check we simulated the reversed situation where $n_{>}$ was kept fixed and $n_{<}$ was allowed to vary in the usual range. As expected the final defect density was constant within error bars, showing no dependence on the value of $\tau_{Q<}$ for negative times. Once again this highlights the fact that the mechanism of defect formation is dictated by what happens after the transition takes place, in vari-

ance with some of the arguments of [1, 2, 3].

V. CONCLUSIONS

If there had been any doubt before, we have shown conclusively that defect density is controlled by the cooling of the system after the critical temperature has been passed. It is true that correlation lengths do freeze in before the transition. However, their defining long-distance behaviour is irrelevant to defect densities, which are controlled by the short-distance behaviour that determines field zeroes.

As we have stressed, transitions with discretely different behaviour before and after the critical temperature of the type that we have examined are unlikely to have direct physical counterparts. However, the transitions in Josephson Junctions provide a more subtle example where behaviour before and after the transition is very different. Before the conductor-superconductor transition we have two bulk conductors, individually amenable to the Zurek analysis of freezing in of correlation lengths [3]. For these, (3) is appropriate, with $\sigma_{<} = 1/4$. However, after the transition we have the Josephson effect, for which field ordering is not determined by the behaviour of the individual superconductors, for which (3) would have given an identical $\sigma_{>} = 1/4$ [3]. Instead, field ordering is constrained by the velocity of light in the oxide, the Swihart velocity [22]. Naively, we could not easily distinguish between the two possibilities since, for idealised symmetric junctions this again gives the same scaling behaviour $\sigma_{>} = 1/4$ [22] after the transition, albeit with a different prefactor. However, for realistic junctions proximity effects and only partial critical slowing-down $\sigma_{<} = 1/4$ enforce $\sigma_{>} = 1/2$ [16]. Empirically, the data is described well by the latter [16], and is not compatible with $\sigma_{<} = 1/4$.

Both the analytical estimates and the numerical simulations presented above suggest strongly that our results should apply to domain formation in generic second-order phase-transitions.

N. D. Antunes was funded by PPARC. P. Gandra was supported by FCT, grant number PRAXIS XXI BD/18432/98. R. J. Rivers would like to acknowledge support from the ESF COSLAB programme.

-
- [1] T.W.B. Kibble, in *Common Trends in Particle and Condensed Matter Physics*, *Physics Reports* **67**, 183 (1980).
[2] W.H. Zurek, *Nature* **317**, 505 (1985), *Acta Physica Polonica* **B24**, 1301 (1993).
[3] W.H. Zurek, *Physics Reports* **276**, Number 4, Nov. 1996.
[4] S. Ducci, P.L. Ramazza, W. González-Viñas, and F.T. Arecchi, *Phys. Rev. Lett.* **83**, 5210 (1999).
[5] R. Monaco, J. Mygind and R.J. Rivers *Phys. Rev. Lett.* **89**, 080603 (2002); *Phys. Rev.* **B 67**, 104506 (2003).
[6] A. Maniv, E. Polturak and G. Koren, *Phys. Rev. Lett.* **91**, 197001 (2003).
[7] C. Bauerle *et al.*, *Nature* **382**, 332 (1996).
[8] V.M.H. Ruutu *et al.*, *Nature* **382**, 334 (1996).
[9] R. Carmi and E. Polturak, *Phys. Rev.* **B 60**, 7595 (1999).
[10] S. Digal, R. Ray and A.M. Srivastava *Phys. Rev. Lett* **83**, 5030 (1999)

- [11] A.J. Gill, R.J. Rivers, *Phys. Rev.*D51, 6949-6958 (1995)
- [12] G. Karra, R.J. Rivers, *Phys. Lett. B* 414, 28-33 (1997)
- [13] G. Karra and R.J. Rivers, *Phys. Rev. Lett.* **81** 3707 (1998).
- [14] R.J. Rivers, *Phys. Rev. Lett.* 84, 1248-1251 (2000)
- [15] E. Moro and G. Lythe, *Phys.Rev.* **E59** R1303 (1999).
- [16] R. Monaco, J. Mygind, M. Aaroe, R.J. Rivers, V.P. Koshelets, cond-mat/0503707, to be published in *Phys. Rev. Lett.*
- [17] P. Laguna and W.H. Zurek, *Phys. Rev.* **D58**, 085021 (1998); P. Laguna and W.H. Zurek, *Phys. Rev. Lett.* **78**, 2519 (1997).
- [18] N. D. Antunes, P. Gandra and R. Rivers, hep-ph/0501168, to be published in *Phys. Rev. D*.
- [19] R.J. Rivers, E. Kavoussanaki and G. Karra, *Condensed Matter Physics*, Volume 3, 133-168 (2000)
- [20] B.I. Halperin, published in *Physics of Defects*, proceedings of Les Houches, Session XXXV, 1980, editors Balian, Kléman and Poirier (North-Holland Press, 1981) p.816.
- [21] F. Liu and G.F. Mazenko, *Phys. Rev.* **B46**, 5963 (1992).
- [22] E. Kavoussanaki, R. Monaco and R.J. Rivers, *Phys. Rev. Lett.* **85**, 3452 (2000). R. Monaco, R.J. Rivers and E. Kavoussanaki, *Journal of Low Temperature Physics* **124**, 85 (2001).